

Original Article

Treatment of contaminated radial fracture in Sprague-Dawley rats by application of a degradable polymer releasing gentamicin

Yuval Ramot^{1†}, Michal Steiner^{2†}, Netanel Amouyal², Yossi Lavie², Guy Klaiman², Abraham J. Domb³, Abraham Nyska^{4*}, and Tal Hagigit⁵

¹ Faculty of Medicine, The Hebrew University of Jerusalem, Israel; The Department of Dermatology, Hadassah Medical Center, POB 12000, Jerusalem, 9112001, Israel

² Envigo CRS (Israel), Einstein Street, 13B, P.O.B 4019, Science Park, Ness Ziona, Israel

³ Institute of Drug Research, School of Pharmacy-Faculty of Medicine, The Hebrew University of Jerusalem, POB 12000, Jerusalem, 9112001 Israel

⁴ Consultant in Toxicologic Pathology, Tel Aviv and Tel Aviv University, Yehuda HaMaccabi 31, Tel Aviv, 6200515, Israel

⁵ Dexcel Pharma Technologies Ltd., 1 Dexcel St., Or-Akiva, 3060000, Israel

Abstract: Fracture-related infections remain a leading cause of morbidity and mortality. We aimed to establish a simple contaminated radial osteotomy model to assess the efficacy of a biodegradable polymer poly(sebacic-co-ricinoleic acid) [p(SA-RA)] containing 20% w/w gentamicin. A unilateral transverse osteotomy was induced in Sprague-Dawley (SD) rats, followed by application of *Staphylococcus aureus* suspension over the fracture. After successfully establishing the contaminated open fracture model, we treated the rats either systemically (intraperitoneal cefuroxime), locally with p(SA-RA) containing gentamicin, or both. Control groups included non-contaminated group and contaminated groups that were either untreated or treated with the polymer alone. After 4 weeks, the bones were subjected to micro-CT scanning and microbiological and histopathology evaluations. Micro-CT analysis revealed similar changes in the group subjected to both local and systemic treatment as in the non-contaminated control group. Lack of detectable bacterial growth was noted in most animals of the group subjected to both local and systemic treatment, and all samples were negative for *S. aureus*. Histopathological evaluation revealed that all treatment modalities containing antibiotics were highly effective in reducing infection and promoting callus repair, resulting in early bone healing. While p(SA-RA) containing gentamicin treatment showed better results than cefuroxime, the combination of local and systemic treatment displayed the highest therapeutic potential in this model. (DOI: 10.1293/tox.2020-0041; J Toxicol Pathol 2021; 34: 11–22)

Key words: osteomyelitis, animal model, efficacy, biodegradability, fracture, Sprague-Dawley (SD) rats

Introduction

Fracture-related infection can be a source of severe complications, including osteomyelitis or septicemia. Furthermore, such infections can result in a delay in bone healing and functional damage that results in increased hospitalization time and healthcare costs¹. Debridement of the open fracture and prolonged antibiotic treatment can still result in infection; indeed, treatment failure is observed in 10–30% of the cases^{2–5}. In addition, prolonged intravenous antibiotic administration (over 6 weeks of treatment) requires the

invasive catheter placement and administration of several doses of antibiotics daily⁶. Thus, management of such infections still poses a medical challenge.

Therefore, the use of local antibiotic delivery methods has frequently been implemented as an adjuvant antimicrobial treatment. Such methods include the use of non-biodegradable materials, such as polymethylmethacrylate (PMMA) beads with gentamicin and PMMA cement impregnated with antibiotics. However, the use of non-biodegradable materials requires an additional surgery to remove them from the implantation site^{7, 8}. Biodegradable materials have been developed, such as gentamicin-impregnated collagen sheets and calcium sulphate, but often result in an uncontrolled release of the antibiotics, and localized hypersensitivity reactions have been observed with their use^{9–12}.

Previous *in vitro* and *in vivo* studies have shown that poly(sebacic-co-ricinoleic acid) (p(SA-RA)) can serve as a convenient and safe biodegradable polymer for the local administration of drugs^{13–15}. The polymer hydrolyses through anhydride cleavage lasting ~7 days to form oligoesters, which are stable for more than 30 days. The short oligomers

Received: 15 June 2020, Accepted: 6 August 2020

Published online in J-STAGE: 31 August 2020

*Corresponding author: A Nyska (e-mail: anyska@bezeqint.net)

†These authors contributed equally to this work.

©2021 The Japanese Society of Toxicologic Pathology

This is an open-access article distributed under the terms of the Creative Commons Attribution Non-Commercial No Derivatives

(by-nc-nd) License. (CC-BY-NC-ND 4.0: <https://creativecommons.org/licenses/by-nc-nd/4.0/>).



encapsulate the drug, from which it is slowly released¹⁴. It was also evaluated as a method for gentamicin administration for the treatment of osteomyelitis^{16–18}, showing good tolerability, favorable local release dynamics, and no signs of inflammatory reaction.

The aim of the current study was to evaluate the efficacy of p(SA-RA) containing 20% w/w gentamicin to treat open radial fracture infection, in an artificially contaminated fracture rat model. This was a two-step study: in the first part we aimed to establish the artificial contaminated open fracture model in the radius bone of male Sprague-Dawley (SD) rats. After establishing the model, it was used to test the efficacy of p(SA-RA) containing gentamicin to treat the infected fracture site in male SD rats, with and without systemic antibiotic administration.

Materials and Methods

Animal husbandry and maintenance

A total of 12 male SD rats, 9 weeks of age at the start of the study, were used for the model establishment study. An additional 60 male rats, 8 weeks of age at the start of the study, were used for the efficacy study. All animals were obtained from Envigo RMS (Israel) Ltd. (Jerusalem, Israel). Animals were housed within a rodent facility in polypropylene cages fitted with solid bottoms and filled with certified commercial wood shavings as bedding material. A certified commercial rodent diet was provided *ad libitum* together with free access to drinking water, supplied to each cage via polyethylene bottles with stainless steel sipper tubes. A temperature of 20–24°C, with a relative humidity of about 30–70%, a 12-h light/12-h dark cycle, and 13 air changes/h was set and maintained automatically.

These studies were performed following an application-form review by the National Council for Animal Experimentation and after receiving approval (No. IL-17-2-55 for the model establishment study phase and No. IL-17-10-356 for the efficacy assessment study phase) that the studies comply with the established rules and regulations set forth. The number of animals used was the minimum that is consistent with scientific integrity and regulatory acceptability, with consideration for the welfare of the animals in terms of the number and extent of procedures to be carried out on each animal. The studies were conducted at Envigo CRS Israel Ltd. (Ness-Ziona, Israel).

Experimental design

For the model establishment study, animals were divided into 2 groups: one group of animals was used as a control group, and the fracture site was not contaminated with bacteria, while in the test group, the fracture site was contaminated with *Staphylococcus aureus* ATCC 29213 (methicillin-sensitive *S. aureus*) (Table 1). For assessment of efficacy of p(SA-RA) containing 20% w/w gentamicin, the animals were divided into 6 groups, as described in Table 2. All animals were sacrificed on day 28.

Surgical procedure and bacterial contamination

Under systemic analgesia (~0.075 mg/kg of buprenorphine injected subcutaneously at the scruff area), local analgesia (lidocaine 2% injected subcutaneously at the site of skin incision), and generalized anesthesia (isoflurane inhalation), the right fore limb of the animals was fixed firmly and a small (~1 cm) longitudinal incision of the skin was made over the antero-lateral aspect of the radius. Minimal soft tissue blunt dissection was performed to reach the underlying radius bone. The entire perimeter of a small segment (~4 mm) of the bone shaft was cleaned of muscle tissue. A surgical spatula was introduced between the radius and the ulna bones to isolate the site of osteotomy. A complete transverse fracture was induced using a 24 mm diamond cutting disc. The site was washed with sterile saline to remove any bone sliver, and the spatula was removed.

Table 1. Constitution of Treatment Groups in the Model Establishment Study

Group No.	No. of animals	Induction of radial fracture	Contamination	Treatment	Observation period
1M	6	Yes	None	None	28 days following fracture induction
2M	6	Yes	Fracture site was left exposed for 10 min	None	
			Unilateral administration of 20 µl of <i>S. Aureus</i> 4.1×10 ⁶ CFU/ml into the fracture site		

CFU, colony forming unit

Table 2. Constitution of Treatment Groups in the p(SA-RA) Containing 20% w/w Gentamicin Efficacy Study

Group No.	No. of animals	Induction of contaminated radial fracture	Treatment	Sacrifice post treatment-initiation
1M	6	No contamination	Untreated control	28 days following fracture induction
2M	6		Fracture site was left exposed for 10 min	
3M	12		Untreated control	
4M	12	Unilateral administration of 20 µl of <i>S. Aureus</i> ~5×10 ⁶ CFU/ml into the fracture site	Application of p(SA-RA)	
5M	12		Application of p(SA-RA) containing 20% w/w gentamicin at the fracture site	
6M	12		Application of p(SA-RA) containing 20% w/w gentamicin at the fracture site & 3 days × twice daily IP injection of cefuroxime	
			3 days × twice daily IP injection of cefuroxime	

Bacterial contamination was induced by a single 20 μ l administration of *S. aureus* over the fracture site prepared and supplied by Aminolab Ltd. (Ness Ziona, Israel). Cell concentrations were 4.1×10^6 colony forming units (CFU)/ml in the model establishment phase and 5.5 to 5.6×10^6 CFU/ml in the efficacy assessment phase. The site was kept exposed for 10 minutes prior to wound closure or application of treatment in the respective groups. *S. aureus* was selected for this study, since it is the most common clinical isolate used in drug discovery research^{19, 20}.

In the efficacy assessment phase, group 3M was subjected to local treatment by application of 0.05 ml of the p(SA-RA) at the fracture site supplied by Dexcel Pharma Technologies Ltd. (Or-Akiva, Israel). Groups 4M and 5M were subjected to local treatment by application of 0.05 ml p(SA-RA) containing 20% w/w gentamicin at the treatment site, supplied by Dexcel Pharma Technologies Ltd. (Or-Akiva, Israel). Group 5M was also subjected to systemic antibiotic treatment in the form of repeated intraperitoneal (IP) injections of 30 mg/kg Cefuroxime (0.4 ml/kg of reconstituted dosing solution, Panpharma Laboratories, Luitré, France), a total of 6 injections, carried out twice daily for 3 successive days. The first injection was carried out on the day of surgery, at the end of the day, to enable robust drug coverage throughout the planned systemic antibiotic treatment period. Group 6M was also subjected to the same systemic treatment under the same regimen. All animals were kept in individual cages for the first week after surgery.

Observations and examinations

Detailed clinical examinations of the animals were carried out once weekly. On all other days, cage-side observations were carried out. Observations included changes in skin, fur, eyes, mucous membranes, occurrence of secretions and excretions (e.g., diarrhea), and autonomic activity (e.g., lacrimation, salivation, piloerection, unusual respiratory pattern). Changes in gait, posture, and response to handling, as well as the presence of peculiar behavior, tremors, convulsions, sleep, and coma were also assessed. Special attention was given to any local reaction at the surgical site. Determination of individual body weights of animals was initially carried out at the randomization procedure, followed by body weight determination on the day of model induction, and at least once weekly thereafter until study termination.

X-ray imaging

All animals' right limbs were subjected to digital X-ray radiography on two perpendicular views, anteroposterior (AP) and lateral (uniformity was kept between animals) under general anesthesia, at one and eight days after surgery in the model establishment study and one day after surgery in the efficacy study. Both AP and lateral radiographs were used to verify the fracture apposition (i.e. the amount of end-to-end contact of the fracture) and alignment (i.e. rotational or angular position) (Supplementary. Fig. 1).

Micro-computed tomography (CT) imaging

The right radius bones of all animals were subjected to micro-CT scanning 1 day prior to study termination (i.e. 27 days post fracture induction) to identify and evaluate the extent of osseous changes. The images (i.e., microtomograms) were analyzed for the following parameters using SkyScan software: periosteal reaction, osteolysis, cortical thickening, fracture line clearance, alignment rate, and any noticeable lesions. The changes were scored, using semi-quantitative grading (0–3), taking into consideration the severity of the changes (0 = No or Unremarkable change, 1 = Mild change, 2 = Moderate change, 3 = Severe change).

Bone excision and fixation

At the end of the observation period, the right radius bones were excised aseptically from all animals in a biological hood. The fur was disinfected with 70% ethanol prior to excision of bones, and equipment was disinfected with 4% w/v Chlorhexidine Gluconate (SEPTAL SCRUB®) and then wiped with ethanol 70%. In order to minimize the chance of bacterial cross contamination between the test groups, the first group that was subjected to bone excision was group 1M. All excised organs were assessed for abnormalities and gross pathological changes.

Half of the animals in each group (i.e., 3 animals/group in model establishment study and groups 1M and 2M in the efficacy assessment phase, and 6 animals/group in groups 3M–6M) were designated for microbiological assessment, whereas the other half were designated for histopathological examination. The muscle and connective tissue were removed from the radius bones designated for microbiological assessment. Each bone was placed in a sterile nylon bag and then crushed with a pestle under sterile conditions. A total of 10 ml of sterile PBS was added to the nylon bag containing the radial fragments. The radius bones from animals designated for histopathological examination were fixed in 10% neutral buffered formalin (approximately 4% formaldehyde solution).

Microbial assessment

Each bone suspension was vortexed and then serial dilutions were prepared and inoculated onto plates of Baird-Parker Agar to determine the staphylococci genus. In the efficacy assessment phase, the bone suspensions were also inoculated onto Tryptic Soy Agar to determine the total bacterial CFU/ml. Confirmation tests for the identification of *S. Aureus* species were performed on colonies obtained on Baird Parker Agar, using coagulase test. The mean number of CFU per milliliter of solution was calculated for all colonies after 48 h of incubation at 37°C. The limit of detection was <10 CFU/ml for a 1:10 dilution.

Histological processing and histopathological evaluation

The radius bones were decalcified and then embedded in paraffin. Thereafter, the block was trimmed at "level 0" (identification of the medullary cavity, represented by the

blue line in Supplementary Fig. 2), the first section (5 microns thickness) was taken for slide preparation, as well as a section 50 microns deep (represented by the green line in Supplementary Fig. 2). This section (represented by the green line) produced a complete longitudinal section of the radius, which enabled observation of the complete length of the medullary cavity. Slides were then stained with hematoxylin and eosin (H&E).

The following parameters were specifically evaluated in the callus area: infection (abscess formation), bone necrosis, periosteal new trabecular bone formation, and intramedullary fibrosis. Histopathological changes were scored where applicable using semi-quantitative grading of five grades (0–4), taking into consideration the severity of the changes (0 = No lesion, 1 = Minimal change, 2 = Mild change, 3 = Moderate change, 4 = Marked change).

Grading of callus repair was performed on a 0–6 scale²¹: 0 = non-union (fibrous tissues), 1 = incomplete cartilage union (cartilage with some fibrous tissues), 2 = complete cartilage union (entirely cartilage), 3 = incomplete bony union with early ossification phase (predominantly cartilage with some trabecular bone), 4 = incomplete bony union with intermediate ossification phase (equal amounts of cartilage and trabecular bone), 5 = incomplete bony union with late ossification phase (predominantly trabecular bone with some cartilage), 6 = complete bony union (entirely bone).

Results

Model establishment study phase

Mortality, clinical signs, and body weights: No mortality occurred in any of the animals throughout the 4 week observation period. During the first week after surgery, 1 animal from group 1M (no contamination) and 4 animals from group 2M (contaminated) avoided using the operated limb. Swelling at the operated limb was further noted in 2 animals from group 1M and in 5 animals from group 2M at a certain observation time point throughout the study period. During weeks 2–3, rigid bulge at the fracture site was felt upon palpation in 3 animals from group 2M.

Both groups had comparable body weight gain at the end of the observation period. A decrease in all animals' body weight was noted in the first few days after surgery; however, by day 10, all animals from the model establishment study had returned to their initial body weight.

X-ray imaging: In the first radiography session of group 1M, perfect apposition was seen in 3 animals and partial apposition in 3 animals. In the animals from group 2M, the extent of apposition was partial in 3 animals and perfect in the remaining 3 animals (Table 3). The second radiography session was performed 8 days post induction. In group 1M, partial apposition was seen in all animals. In group 2M, perfect apposition was seen in 1 animal, partial in 2 animals, and side to side apposition in 3 animals.

Microbial evaluation: The total number of CFU/ml in group 1M ranged between 1.7×10^1 and 2.83×10^2 , whereas in

group 2M it reached a 10^3 scale in 2/3 animals, and in the third animal it was 9.3×10^1 (Table 4).

Due to atypical *Staphylococcal* growth identified in the plates of samples from group 1M, a coagulase test was performed on colonies obtained on Baird Parker Agar for identification of *S. aureus*. The test results confirmed that the microorganism colonies in group 1M were not *S. aureus* and confirmed that group 2M colonies represented *S. aureus* colonies.

Micro-CT imaging: There were differences in the extent of observed changes between the non-contaminated group vs. the bacteria contaminated group. The changes mainly consisted of osteolysis, fracture line clearance, and presence of sequestrum (Table 5). The changes in group 2M were indicative of severe response to the induction of bacterial contamination. Nevertheless, the periosteal reaction in both groups ranged between moderate and severe and reflects a surgical-related effect.

Macroscopic and microscopic findings: Macroscopically, no apparent differences were noted in the radius bones of animals from both groups. In 3 animals from group 2M, a nodule (~2–3 mm in diameter) consistent with suppurative material content at the subcutaneous tissue over the fracture site was noted.

Microscopically, the main characteristics of the changes observed in the samples from group 1M consisted of callus repair – scored as Grade 3 (i.e., incomplete bony union with early ossification phase - predominantly cartilage with some trabecular bone) (Table 6 and Fig. 1). Generally, there was minimal or no cortical bone damage. In contrast, the main characteristics of the changes observed in group 2M included the presence of abscesses within the callus, related to the bacterial suspension administered directly over the fractured bone, associated with significant delay in callus maturation (i.e., scored as Grade 1 - incomplete cartilage union - cartilage with some fibrous tissues) (Table 6 and Fig. 2). In addition, a range of cortical bone destruction (i.e., minimal to moderate) was noted at the site of the callus formation.

Efficacy assessment study phase

Mortality, clinical signs, and body weights: No mortality occurred in any of the animals throughout the 4 week observation period. Avoidance of using the operated limb was the most common observation and was more common in groups 3M and 4M particularly during the second week of the observation period (Supplementary Table 1). Decrease in all animals' body weight was noted during the first week post-fracture induction; however, by study day 9, all animals from the efficacy assessment study regained their initial body weight and demonstrated expected growth pattern until the end of the observation period (Supplementary Table 2).

X-ray imaging: Among 60 animals, perfect apposition was seen in 26 animals, partial apposition in 32 animals, and side to side apposition in 2 animals, both from group 4M (Table 7). Each group included animals with partial and

Table 3. Extent of Bone Apposition in the Model Establishment Phase (1- and 8-days Post-fracture Induction)

Group No.	Extent of apposition (perfect/partial/ side to side)	Time post fracture induction (number affected/ total number of animals)	
		1 day	8 days
1M	Perfect	3/6	0/6
	Partial	3/6	6/6
	Side to side	0/6	0/6
2M	Perfect	3/6	1/6
	Partial	3/6	2/6
	Side to side	0/6	3/6

1M = No contamination; 2M = *S. Aureus*.

Table 4. Microbial Results in the Model Establishment Phase (28 Days Post-fracture Induction)

Group No.	CFU/ml	Coagulase test
1M	8.1×10 ¹	Negative
	2.83×10 ²	Negative
	1.7×10 ¹	Negative
2M	6.4×10 ³	Positive
	9.3×10 ¹	Positive
	1.2×10 ³	Positive

1M = No contamination; 2M = *S. Aureus*.

Table 5. Incidence and Median micro-CT Results in the Model Establishment Phase (27 Days Post-fracture Induction)

Group No.		Observation						
		Osteolysis	Periosteal reaction	Bone sclerosis	Cortical thickening	Fracture line clearance	Alignment rate	Sequestrum
1M	Median	1	2	1	1.5	1	1	1/6
	Incidence	5/6	6/6	6/6	6/6	5/6	4/6	
	Min	0	2	1	1	0	0	
	Max	2	3	3	2	2	1	
2M	Median	2.5	2	1	2	2.5	0	5/6
	Incidence	6/6	6/6	6/6	6/6	6/6	1/6	
	Min	2	2	1	1	2	0	
	Max	3	3	3	3	3	1	

0 = No or unremarkable changes; 1 = Mild changes; 2 = Moderate changes; 3 = Severe changes. Sequestrum= free bony fragment. SD, standard deviation. 1M = No contamination; 2M = *S. Aureus*.

Table 6. Mean Severity and Incidence of Histopathological Findings Observed in the Model Establishment Phase (28 Days Post-fracture Induction)

Organ/Tissue	Histopathological findings (number affected / total number of animals)	
	Group 1M	Group 2M
	n=3	n=3
Radius-Callus area		
Abscess formation	0.0 (3/3)	2.3 (3/3)
Destruction of cortical bone	0.3 (1/3)	2.0 (3/3)
Periosteal new trabecular bone formation	3.0 (3/3)	3.0 (3/3)
Intramedullary fibrosis in the callus area	1.0 (3/3)	1.7 (3/3)
Callus repair	3.0 (3/3)	1.0 (3/3)

Score of changes: 0 = No lesion, 1 = Minimal change, 2 = Mild change, 3 = Moderate change, 4 = Severe change. 1M = No contamination; 2M = *S. Aureus*.

perfect apposition, with no apparent effect of the local application of p(SA-RA) or p(SA-RA) containing 20% w/w gentamicin on the fracture's apposition (Supplementary Fig. 3).

Microbial evaluation: All animals from group 1M were negative for *S. aureus*, while all animals from group 2M were positive, as expected. Non-specific bacterial growth (i.e., either Staphylococci or other non-*S. aureus* bacteria) was identified in 2 animals from group 1M and was re-

Table 7. Extent of Bone Apposition in the Efficacy Evaluation Phase (1-day Post-fracture Induction)

Group No.	Extent of apposition (perfect/partial/side to side)	1 day post fracture induction
		(number affected / total number of animals)
1M	Perfect	3/6
	Partial	3/6
	Side to Side	0/6
2M	Perfect	4/6
	Partial	2/6
	Side to Side	0/6
3M	Perfect	2/12
	Partial	10/12
	Side to Side	0/12
4M	Perfect	2/12
	Partial	8/12
	Side to Side	2/12
5M	Perfect	6/12
	Partial	6/12
	Side to Side	0/12
6M	Perfect	9/12
	Partial	3/12
	Side to Side	0/12

1M = Sham; 2M = Untreated control; 3M = p(SA-RA); 4M = p(SA-RA) containing 20% w/w gentamicin; 5M = p(SA-RA) containing 20% w/w gentamicin + IP cefuroxime; 6M = IP cefuroxime.

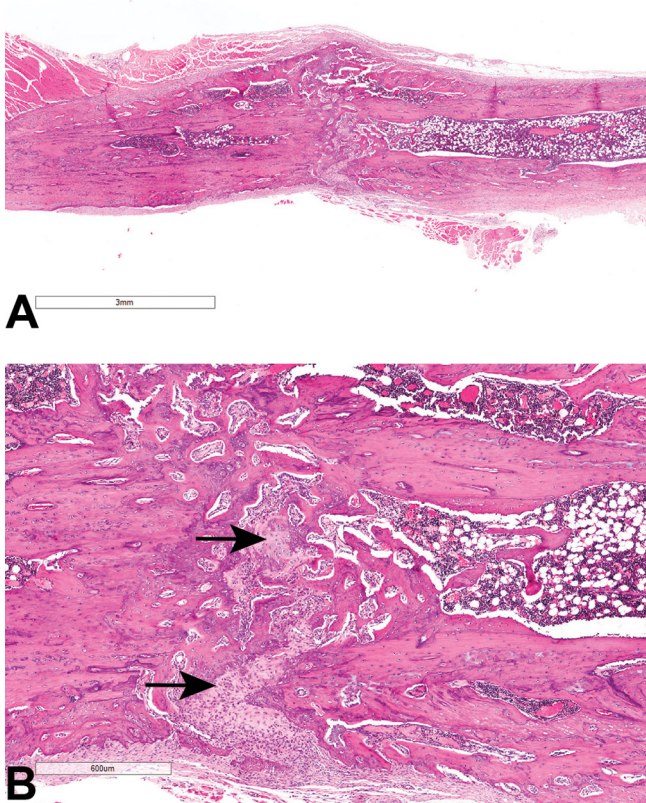


Fig. 1. A: Low magnification. B: Higher magnification of the same field shown in A. Section of the radius from animal of Group 1M (model establishment phase, sacrificed on Day 28), showing grade 3 of callus repair (i.e., incomplete bony union with early ossification phase—predominantly cartilage with some trabecular bone). Arrows indicate the cartilage component of the callus.

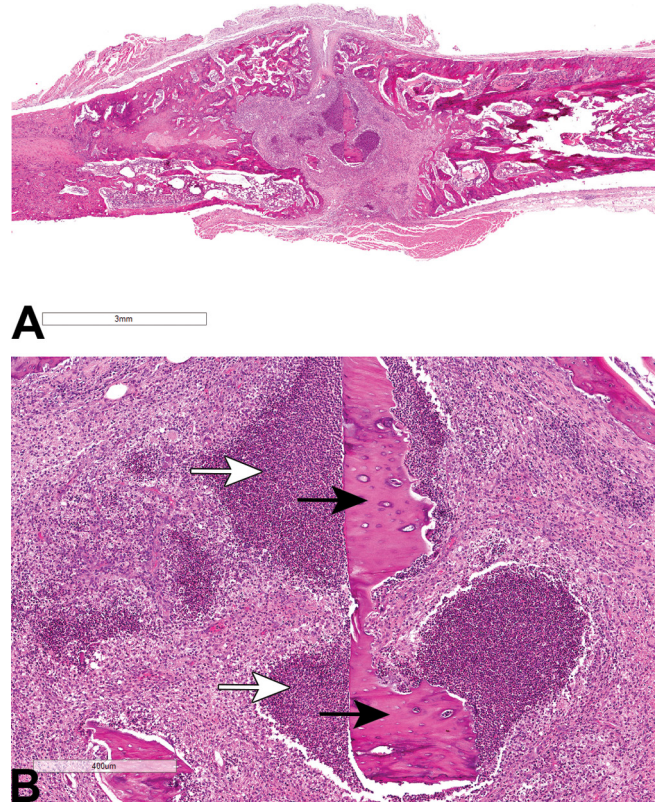


Fig. 2. A: Low magnification. B: Higher magnification of the same field shown in A. Section of the radius from animal of Group 2M (model establishment phase, sacrificed on Day 28), showing grade 1 of callus repair (i.e., incomplete cartilage union—cartilage with some fibrous tissues). Black arrows indicate the necrotic bone. Open arrows indicate the presence of suppurative inflammation within the callus.

garded as an incidental finding, which might be related to exposure of the wound to air for ten minutes during fracture induction, or to the non-sterile manner of bone excision or handling of the bone suspension (Table 8).

Micro-CT imaging: The extent and differences in osteolysis, sequestrum incidence, and fracture line clearance scores between groups 1M (non-contaminated, untreated control) and 2M (contaminated, untreated control) demonstrate the robustness of this model (Table 9, Supplementary Fig. 4). Group 3M (contaminated, vehicle control) displayed similar median values as in group 2M, while the extent of changes in groups 4M [contaminated, local treatment with p(SA-RA) containing 20% w/w gentamicin] and 6M (contaminated, systemic treatment) was comparable, and is indicative of a balance between bone infection and healing process. The combination of local and systemic treatment (group 5M) achieved the best results, which were similar to the results observed in the non-contaminated, untreated control group.

Macroscopic and microscopic findings: Macroscopic findings were seen in 4/6 animals from group 2M and in 5/12 animals from group 3M. The findings included firm

tissue bridging between the ulna and radius bones in 2/6 animals from group 2M and in 4/12 animals from group 3M; nodule consistent with suppurative material content at the subcutaneous tissue over the fracture site in 2/6 animals from group 2M and in 3/12 animals from group 3M; and abscess-like lesion at the fracture site between the radial fragments in 1/12 animals from group 3M. No gross lesions were seen in any of the animals from groups 1M, 4M, 5M, and 6M. No gross lesions were seen in the lungs of all animals from every study group.

In all groups treated with any one of the therapeutic modalities (i.e., groups 4M, 5M, and 6M), the analysis of the individual data demonstrated a highly effective capacity to considerably reduce infection and promote callus repair, resulting in early bone healing compared to both contaminated untreated and vehicle control groups (i.e., groups 2M and 3M).

The bone fracture site in group 1M (i.e., non-contaminated, untreated control) indicated a trend for almost complete and/or complete healing of the fracture area, without any local complications (i.e., inflammation) (Table 10 and Fig. 3). The bone fracture site in groups 2M and 3M indi-

Table 8. Microbial* Results in the Efficacy Evaluation Phase (28 Days Post-fracture Induction)

Group No.	Total bacteria	Staphylococci species	Coagulase test
	CFU/ml	CFU/ml	
1M	<1×10 ¹	<1×10 ¹	Not applicable
	1.4×10 ⁴	7.7×10 ³	Negative
	1.5×10 ¹	<1×10 ¹	Negative
2M	8.2×10 ³	6.2×10 ³	Positive
	4.7×10 ³	3.7×10 ³	Positive
	1.0×10 ⁴	1.3×10 ⁴	Positive
3M	1.9×10 ⁴	1.7×10 ⁴	Positive
	1.4×10 ³	7.4×10 ²	Positive
	2.9×10 ³	8.9×10 ²	Positive
	7.5×10 ³	2.6×10 ³	Positive
	1.6×10 ³	1.4×10 ³	Positive
4M	1.2×10 ⁴	1.2×10 ⁴	Positive
	<1×10 ¹	1.5×10 ²	Negative
	2.7×10 ⁴	2.4×10 ⁴	Negative
	1.6×10 ²	1.6×10 ²	Negative
	<1×10 ¹	<1×10 ¹	Not applicable
	<1×10 ¹	<1×10 ¹	Not applicable
5M	2.3×10 ²	90	Negative
	<1×10 ¹	<1×10 ¹	Not applicable
	<1×10 ¹	<1×10 ¹	Not applicable
	1.6×10 ²	1.5×10 ²	Negative
	<1×10 ¹	<1×10 ¹	Not applicable
	<1×10 ¹	<1×10 ¹	Not applicable
6M	8.5×10 ¹	65	Negative
	1.5×10 ³	1.5×10 ³	Positive
	4.7×10 ³	5.2×10 ³	Positive
	<1×10 ¹	<1×10 ¹	Not applicable
	<1×10 ¹	<1×10 ¹	Not applicable
	<1×10 ¹	<1×10 ¹	Not applicable

*Each bone suspension sample was inoculated onto two different media, enabling propagation of total bacteria (Tryptic Soy Agar), or Staphylococci (Baird Parker Agar). The bacterial propagation potential is represented by the order of magnitude of total CFU/ml on each growth medium and was extrapolated based on several inoculated dilutions of bone suspension in duplicates. Therefore, where a sample shows the same order of magnitude, or up to half-log difference, of CFU/ml on both media, it is regarded as staphylococcal dominance rather than other bacterial growth. Similarly, bacteria count in Baird Parker Agar may be greater than the count in Tryptic Soy Agar, due to relative staphylococcal growth predominance over the preferred medium. 1M = Sham; 2M = Untreated control; 3M = p(SA-RA); 4M = p(SA-RA) containing 20% w/w gentamicin; 5M = p(SA-RA) containing 20% w/w gentamicin + IP cefuroxime; 6M = IP cefuroxime.

cated no bone healing of the fracture, associated with the presence of local intramedullary necrotic bone and presence of intramedullary abscess formation (Table 10 and Fig. 4 and 5). The bone fracture site in groups 4M, 5M, and 6M indicated almost complete and/or complete healing of the fracture area, without any local complications (i.e., inflammation) (Table 10 and Fig. 6–8). Occasionally, minimal focal remnants of necrotic bone and/or minimal focal remnants of abscess were identified. However, as these changes were strictly circumscribed, it was not considered important, simply a reflection of the process of normal fracture

healing and not indicative of disease or infection.

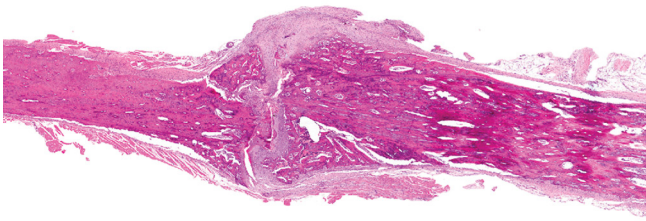
Discussion

The first phase of this study was to establish a reliable and reproducible model for *S. aureus* artificially contaminated open fracture. An establishment of preclinical *in vivo* models in a controlled environment is a critical step prior to application of any novel intervention, avoiding external variables that may interfere with efficacy and safety evaluation^{19, 22}. This can be achieved by minimizing the need for surgical intervention and reducing the impact on animals' functional/mechanical competence. An osteotomy model improves reproducibility among multiple animals in comparison to induction of traumatic fracture. The radius bone exhibits several characteristics which makes it suitable as a testing model. The body weight load in rats is mainly supported by the hind limbs; therefore, the mechanical burden at the radial fracture site is relatively low. Furthermore, the surrounding muscles and the parallel ulna bone contributes to the mechanical support of the fracture without additional fixators, such as (1) intramedullary pin which may lead to microbial anchorage (biofilm), or (2) external fixator which necessitates increasing the extent of the surgical intervention. The limited exposure time of 10 min, in which the wound is left open prior to application of the local treatment and/or closure of skin, shortened the anesthesia time as well. The contaminated radial open osteotomy model enables a reduction in the number of animals and still produces reliable data with minimal background noise.

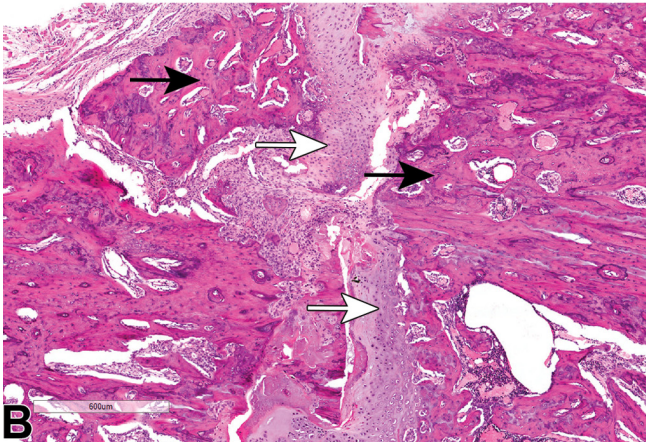
In our study, we have utilized several evaluation methods, including histopathological, micro-CT and microbiological examinations. Microbial examinations showed *S. aureus* growth, while micro-CT scans revealed severe response to the induction of bacterial contamination; additionally, a significant delay in callus maturation was evident on histopathology. Taken together, these results confirm successful establishment of the artificial contaminated open fracture model of the radius bone in male SD rats.

After establishment of the fracture model, it was used to assess the effectiveness of p(SA-RA) containing 20% w/w gentamicin in eliminating the bacteria and reducing the negative consequences of osteomyelitis on bone healing. Gentamicin is an aminoglycoside that is commonly used in both human and animal models to treat or prevent osteomyelitis due to thermostability and wide antibacterial spectrum^{23–26}. In this study, we used IP injection of cefuroxime as an active control for p(SA-RA) containing 20% w/w gentamicin, and we also incorporated non-contaminated control, contaminated untreated control, and treatment with the biodegradable polymer alone (p(SA-RA)).

The p(SA-RA) containing 20% w/w gentamicin is a biodegradable gel that has also been previously tested in animal models and *in vitro* for the treatment of osteomyelitis^{17, 18}. The use of biodegradable materials is gaining a lot of interest in the medical field in general, and in the orthopedic field in particular. Indeed, data on the use of such materials in preclinical studies are accumulating, providing more

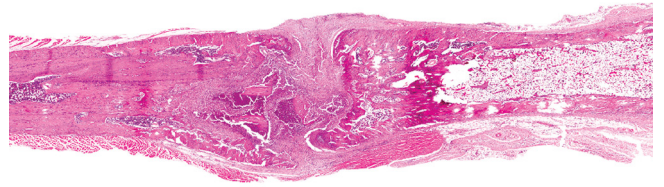


A 

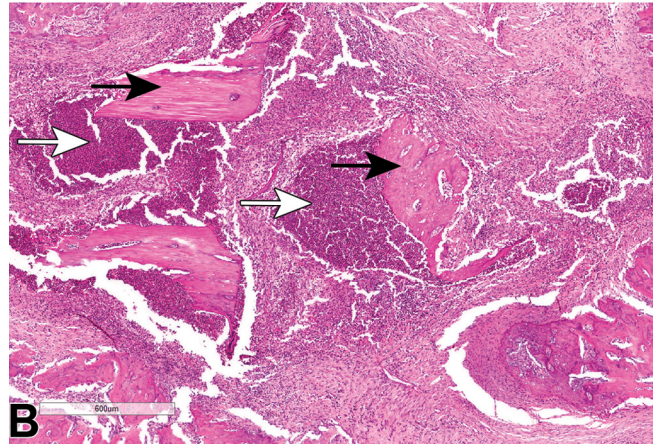


B 

Fig. 3.

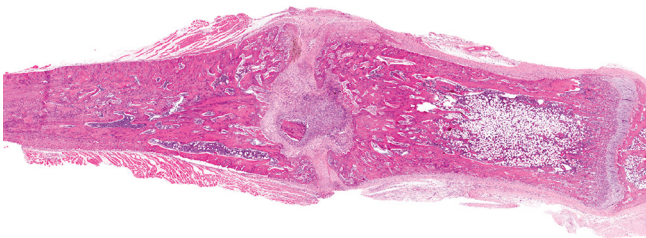


A 

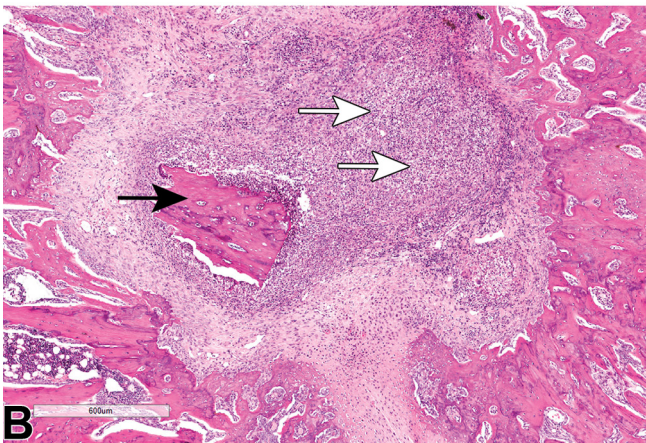


B 

Fig. 4.

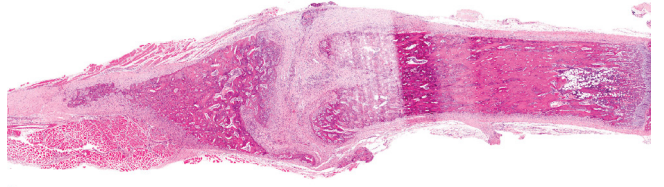


A 

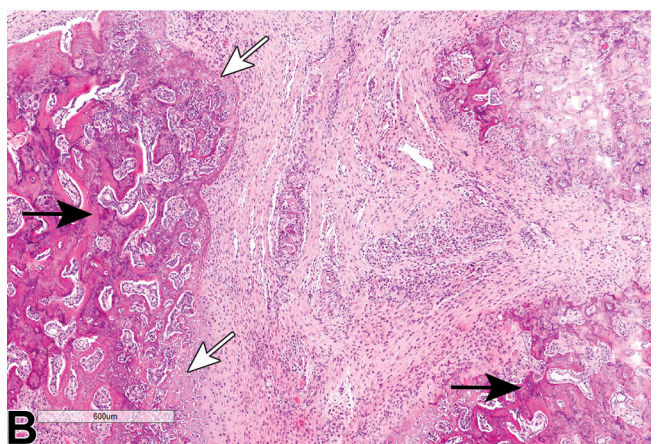


B 

Fig. 5.



A 



B 

Fig. 6.

- Fig. 3.** A: Low magnification. B: Higher magnification of the same field shown in A. Section of the radius from animal of Group 1M (efficacy assessment phase) showing grade 5 healing score—there is incomplete bony union with a late ossification phase (predominantly trabecular bone with some cartilage). Black arrow indicates intramedullary new trabecular bone formation. Open arrows indicate intramedullary cartilage.
- Fig. 4.** A: Low magnification. B: Higher magnification of the same field shown in A. Section of the radius from animal of Group 2M (efficacy assessment phase) showing healing score grade 0—non-union (fibrous tissues) is seen. Open arrow indicates abscess formation. Black arrows indicate necrotic bone.
- Fig. 5.** A: Low magnification. B: Higher magnification of the same field shown in A. Section of the radius from animal of Group 3M (efficacy assessment phase) showing healing score grade 0—non-union (fibrous tissues) can be seen. Open arrows indicate abscess formation. Black arrow indicates necrotic bone.
- Fig. 6.** A: Low magnification. B: Higher magnification of the same field shown in A. Section of the radius from animals of Group 4M (efficacy assessment phase) showing healing scored grade 4—there is incomplete bony union with intermediate ossification phase (equal amounts of cartilage and trabecular bone). Open arrows indicate intramedullary cartilage formation. Black arrows indicate intramedullary new bone formation.

Table 9. Incidence and Median micro-CT Results in the Efficacy Evaluation Phase (28 Days Post-fracture Induction)

Group No.		Observation						
		Osteolysis	Periosteal reaction	Bone sclerosis	Cortical thickening	Fracture line clearance	Alignment rate	Sequestrum
1M	Median	0	2	1	1.5	0.5	0	
	Incidence	2/6	6/6	6/6	6/6	3/6	2/6	
	Min	0	1	1	1	0	0	1/6
	Max	1	3	2	2	1	1	
2M	Median	3	2	1	1	3	0	
	Incidence	6/6	6/6	4/6	4/6	6/6	0/6	
	Min	2	1	0	0	1	0	6/6
	Max	3	3	1	2	3	0	
3M	Median	2	3	1.5	0.5	2.5	0	
	Incidence	12/12	12/12	12/12	6/12	12/12	4/12	
	Min	2	2	1	0	2	0	12/12
	Max	3	3	2	1	3	2	
4M	Median	1	3	1	1	1	1	
	Incidence	8/12	12/12	11/12	8/12	9/12	7/12	
	Min	0	2	0	0	0	0	5/12
	Max	3	3	2	2	3	3	
5M	Median	0	2	1	1	1	1	
	Incidence	5/12	12/12	12/12	12/12	8/12	8/12	
	Min	0	1	1	1	0	0	0/12
	Max	2	2	2	2	2	3	
6M	Median	1	2	1.5	1	0.5	0	
	Incidence	7/12	12/12	12/12	9/12	6/12	2/12	
	Min	0	1	1	0	0	0	2/12
	Max	3	3	3	2	3	3	

0 = No or unremarkable changes; 1 = Mild changes; 2 = Moderate changes; 3 = Severe changes. Sequestrum = free bony fragment. SD, standard deviation. 1M = Sham; 2M = Untreated control; 3M = p(SA-RA); 4M = p(SA-RA) containing 20% w/w gentamicin; 5M = p(SA-RA) containing 20% w/w gentamicin + IP cefuroxime; 6M = IP cefuroxime.

knowledge on the expected tissue changes associated with their use^{27–32}. However, it is essential to gain more information on the use of such materials in a wider array of animal models and in different tissues.

Microbial examinations revealed that administration of p(SA-RA) containing 20% w/w gentamicin led to excellent culture assessments, with no growth of *S. aureus* in any of the samples; however, minimal staphylococcal growth was noted in 4/6 samples. The best results were achieved with

the combination of p(SA-RA) containing 20% w/w gentamicin and IP injection of cefuroxime, resulting in negative growth in 4/6 samples and minimal growth in 2/6 samples, all negative for *S. aureus*. Notably, in group 6M (contaminated, systemic treatment), bacteria growth was noted in 2/6 samples, which were also positive for *S. aureus*. This finding shows that the systemic treatment by itself, as administered in this study, was not completely effective against the induced infection, and was also less effective than p(SA-RA)

Table 10. Mean Severity and Incidence of Histopathological Findings Observed in the Efficacy Evaluation Phase (28 Days Post-fracture Induction)

Organ/Tissue	Histopathological findings (number affected/ total number of animals)					
	Group 1M n=3	Group 2M n=3	Group 3M n=6	Group 4M n=6	Group 5M n=6	Group 6M n=6
Radius–Callus area						
Abscess formation	0.0 (3/3)	2.0 (3/3)	2.3 (6/6)	0.3 (2/6)	0.0 (6/6)	0.2 (1/6)
Destruction of cortical bone (necrosis; sequestra)	0.0 (3/3)	2.0 (3/3)	1.5 (5/6)	0.3 (2/6)	0.7 (6/6)	0.0 (6/6)
Periosteal new trabecular bone formation	0.0 (3/3)	0.0 (3/3)	0.7 (3/6)	0.0 (6/6)	0.0 (6/6)	0.2 (1/6)
Intramedullary fibrosis in the callus area	1.0 (2/3)	2.7 (3/3)	3.2 (6/6)	2.0 (6/6)	1.3 (5/6)	1.0 (2/6)
Intramedullary new trabecular bone formation	3.0 (3/3)	1.3 (3/3)	0.8 (4/6)	2.5 (6/6)	3.0 (6/6)	2.8 (6/6)
Intramedullary new cartilage formation	1.0 (2/3)	0.0 (3/3)	1.2 (4/6)	1.8 (6/6)	1.8 (5/6)	1.5 (4/6)
Callus repair	5.0 (3/3)	0.0 (3/3)	0.3 (1/6)	3.8 (6/6)	4.5 (6/6)	4.0 (6/6)

Score of changes: 0 = No lesion, 1 = Minimal change, 2 = Mild change, 3 = Moderate change, 4 = Severe change. 1M = Sham; 2M = Untreated control; 3M = p(SA-RA); 4M = p(SA-RA) containing 20% w/w gentamicin; 5M = p(SA-RA) containing 20% w/w gentamicin + IP cefuroxime; 6M = IP cefuroxime.

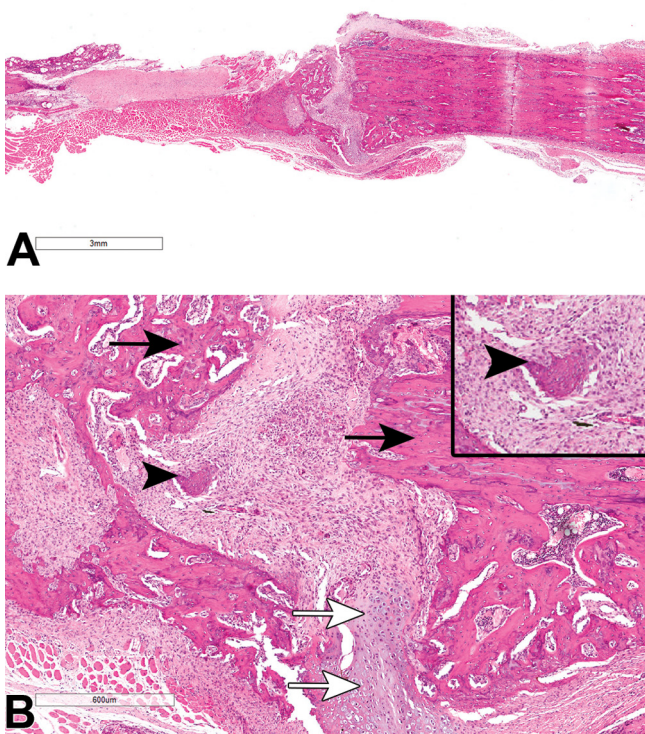


Fig. 7. A: Low magnification. B: Higher magnification of the same field shown in A. Section of the radius from animal of Group 5M (efficacy assessment phase) showing healing scored grade 4—there is incomplete bony union with intermediate ossification phase (equal amounts of cartilage and trabecular bone). Open arrows indicate intramedullary cartilage formation. Black arrows indicate intramedullary new bone formation. Short arrow indicates bone necrosis (also shown in inset, higher magnification).

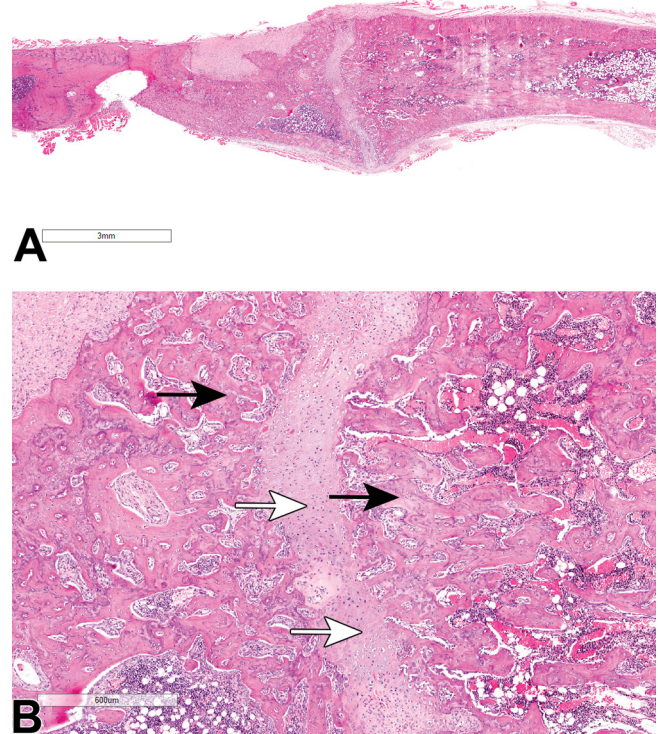


Fig. 8. A: Low magnification. B: Higher magnification of the same field shown in A. Section of the radius from animal of Group 6M (efficacy assessment phase) showing healing scored grade 5—there is incomplete bony union with late ossification phase (predominantly trabecular bone with some cartilage). Black arrows indicate intramedullary new bone formation. Open arrows indicate intramedullary cartilage formation.

containing 20% w/w gentamicin alone. Non-specific staphylococcal bacterial growth was also identified in 2/6 animals from group 1M (i.e., non-contaminated, untreated control)

and, thus, is regarded as background growth, which might be related to exposure of the wound to air for ten minutes during fracture induction, or due to contamination during bone excision or handling of the bone suspension.

Osteolysis was the main micro-CT measure of osseous

change in this model, whereas all other parameters represent processes that are amplified when bacterial infections are involved. These features are either secondary (e.g., clearance of fracture line, sequestrum existence) or consequences that could have been affected by the array of experimental conditions, surgical intervention, lack of bone fixator, animal restraint, extent of local edema, etc. (e.g., periosteal reaction, cortical thickening, bone sclerosis). The results of the ex-vivo micro-CT were consistent with the microbiologic evaluations, showing that the combination of p(SA-RA) containing 20% w/w gentamicin and IP injection of cefuroxime comprises the most effective treatment modality in this model. Histopathological evaluation showed almost complete and/or complete healing of the fracture area, without any local complications (i.e. inflammation), in all the different treatment modalities (groups 4M–6M).

This study has limitations, including the use of only one animal model, limited soft tissue damage, and a follow-up period of only 28 days. However, based on all the different evaluation methods in this model (micro-CT imaging, histopathological and microbiological findings), it is evident that each of the therapeutic modalities, either systemically, by standard regimen of antibiotic agent, locally, by application of p(SA-RA) containing 20% w/w gentamicin, or by their combination, possesses a high capacity to considerably reduce infection and promote callus repair. However, our data point to the fact that the combination of local and systemic treatment has the highest therapeutic potential when compared to the other treatment modalities. These findings indicate that further evaluation of p(SA-RA) containing 20% w/w gentamicin in subsequent in vivo models is a worthwhile endeavor; also, the results are encouraging regarding the future use of this compound in clinical trials in humans.

Disclosure of Potential Conflicts of Interest: Tal Hagigit is an employee of Dexcel Pharma Technologies Ltd. The study was funded by Dexcel Pharma Technologies Ltd., Or-Akiva, Israel.

References

1. Thakore RV, Greenberg SE, Shi H, Foxx AM, Francois EL, Prablek MA, Nwosu SK, Archer KR, Ehrenfeld JM, Obremsky WT, and Sethi MK. Surgical site infection in orthopedic trauma: A case-control study evaluating risk factors and cost. *J Clin Orthop Trauma*. **6**: 220–226. 2015. [[Medline](#)] [[CrossRef](#)]
2. Berkes M, Obremsky WT, Scannell B, Ellington JK, Hymes RA, Bosse M. Southeast Fracture Consortium. Maintenance of hardware after early postoperative infection following fracture internal fixation. *J Bone Joint Surg Am*. **92**: 823–828. 2010. [[Medline](#)] [[CrossRef](#)]
3. Jennison T, McNally M, and Pandit H. Prevention of infection in external fixator pin sites. *Acta Biomater*. **10**: 595–603. 2014. [[Medline](#)] [[CrossRef](#)]
4. O'Brien CL, Menon M, and Jomha NM. Controversies in the management of open fractures. *Open Orthop J*. **8**: 178–184. 2014. [[Medline](#)] [[CrossRef](#)]
5. Tschudin-Sutter S, Frei R, Dangel M, Jakob M, Balmelli C, Schaefer DJ, Weisser M, Elzi L, Battegay M, and Widmer AF. Validation of a treatment algorithm for orthopaedic implant-related infections with device-retention-results from a prospective observational cohort study. *Clin Microbiol Infect*. **22**: 457.e1–457.e9. 2016. [[Medline](#)] [[CrossRef](#)]
6. Costerton JW. Biofilm theory can guide the treatment of device-related orthopaedic infections. *Clin Orthop Relat Res*. (437): 7–11. 2005. [[Medline](#)] [[CrossRef](#)]
7. Gogia JS, Meehan JP, Di Cesare PE, and Jamali AA. Local antibiotic therapy in osteomyelitis. *Semin Plast Surg*. **23**: 100–107. 2009. [[Medline](#)] [[CrossRef](#)]
8. Stańczyk M, and van Rietbergen B. Thermal analysis of bone cement polymerisation at the cement-bone interface. *J Biomech*. **37**: 1803–1810. 2004. [[Medline](#)] [[CrossRef](#)]
9. El-Husseiny M, Patel S, MacFarlane RJ, and Haddad FS. Biodegradable antibiotic delivery systems. *J Bone Joint Surg Br*. **93**: 151–157. 2011. [[Medline](#)] [[CrossRef](#)]
10. Friess W. Collagen–biomaterial for drug delivery. *Eur J Pharm Biopharm*. **45**: 113–136. 1998. [[Medline](#)] [[CrossRef](#)]
11. Hing KA, Wilson LF, and Buckland T. Comparative performance of three ceramic bone graft substitutes. *Spine J*. **7**: 475–490. 2007. [[Medline](#)] [[CrossRef](#)]
12. ter Boo GJ, Grijpma DW, Moriarty TF, Richards RG, and Eglin D. Antimicrobial delivery systems for local infection prophylaxis in orthopedic- and trauma surgery. *Biomaterials*. **52**: 113–125. 2015. [[Medline](#)] [[CrossRef](#)]
13. Haim-Zada M, Basu A, Hagigit T, Schlinger R, Grishko M, Kraminsky A, Hanuka E, and Domb AJ. Alternating poly(ester-anhydride) by insertion polycondensation. *Biomacromolecules*. **17**: 2253–2259. 2016. [[Medline](#)] [[CrossRef](#)]
14. Haim-Zada M, Basu A, Hagigit T, Schlinger R, Grishko M, Kraminsky A, Hanuka E, and Domb AJ. Stable polyanhydride synthesized from sebacic acid and ricinoleic acid. *J Control Release*. **257**: 156–162. 2017. [[Medline](#)] [[CrossRef](#)]
15. Shikanov A, Vaisman B, Krasko MY, Nyska A, and Domb AJ. Poly(sebacic acid-co-ricinoleic acid) biodegradable carrier for paclitaxel: in vitro release and in vivo toxicity. *J Biomed Mater Res A*. **69**: 47–54. 2004. [[Medline](#)] [[CrossRef](#)]
16. Brin YS, Golenser J, Mizrahi B, Maoz G, Domb AJ, Pedada S, Tuvia S, Nyska A, and Nyska M. Treatment of osteomyelitis in rats by injection of degradable polymer releasing gentamicin. *J Control Release*. **131**: 121–127. 2008. [[Medline](#)] [[CrossRef](#)]
17. Brin YS, Nyska A, Domb AJ, Golenser J, Mizrahi B, and Nyska M. Biocompatibility of a polymeric implant for the treatment of osteomyelitis. *J Biomater Sci Polym Ed*. **20**: 1081–1090. 2009. [[Medline](#)] [[CrossRef](#)]
18. Krasko MY, Golenser J, Nyska A, Nyska M, Brin YS, and Domb AJ. Gentamicin extended release from an injectable polymeric implant. *J Control Release*. **117**: 90–96. 2007. [[Medline](#)] [[CrossRef](#)]
19. Reizner W, Hunter JG, O'Malley NT, Southgate RD, Schwarz EM, and Kates SL. A systematic review of animal models for *Staphylococcus aureus* osteomyelitis. *Eur Cell Mater*. **27**: 196–212. 2014. [[Medline](#)] [[CrossRef](#)]
20. Soni I, Chakrapani H, and Chopra S. Draft genome sequence of methicillin-sensitive *Staphylococcus aureus*

- ATCC 29213. *Genome Announc.* **3**: e01095-15. 2015. [[Medline](#)] [[CrossRef](#)]
21. Allen HL, Wase A, and Bear WT. Indomethacin and aspirin: effect of nonsteroidal anti-inflammatory agents on the rate of fracture repair in the rat. *Acta Orthop Scand.* **51**: 595–600. 1980. [[Medline](#)] [[CrossRef](#)]
 22. Vanvelk N, Morgenstern M, Moriarty TF, Richards RG, Nijs S, and Metsemakers WJ. Preclinical in vivo models of fracture-related infection: a systematic review and critical appraisal. *Eur Cell Mater.* **36**: 184–199. 2018. [[Medline](#)] [[CrossRef](#)]
 23. Cibor U, Krok-Borkowicz M, Brzychczy-Włoch M, Rumian Ł, Pietryga K, Kulig D, Chrzanowski W, and Pamuła E. Gentamicin-loaded polysaccharide membranes for prevention and treatment of post-operative wound infections in the skeletal system. *Pharm Res.* **34**: 2075–2083. 2017. [[Medline](#)] [[CrossRef](#)]
 24. Diefenbeck M, Schrader C, Gras F, Mückley T, Schmidt J, Zankovych S, Bossert J, Jandt KD, Völpel A, Sigusch BW, Schubert H, Bischoff S, Pfister W, Edel B, Faucon M, and Finger U. Gentamicin coating of plasma chemical oxidized titanium alloy prevents implant-related osteomyelitis in rats. *Biomaterials.* **101**: 156–164. 2016. [[Medline](#)] [[CrossRef](#)]
 25. Liu D, He C, Liu Z, and Xu W. Gentamicin coating of nanotubular anodized titanium implant reduces implant-related osteomyelitis and enhances bone biocompatibility in rabbits. *Int J Nanomedicine.* **12**: 5461–5471. 2017. [[Medline](#)] [[CrossRef](#)]
 26. Shah MQ, Zardad MS, Khan A, Ahmed S, Awan AS, and Mohammad T. Surgical site infection in orthopaedic implants and its common bacteria with their sensitivities to antibiotics, in open reduction internal fixation. *J Ayub Med Coll Abbottabad.* **29**: 50–53. 2017. [[Medline](#)]
 27. Bergsma JE, de Bruijn WC, Rozema FR, Bos RR, and Boering G. Late degradation tissue response to poly(L-lactide) bone plates and screws. *Biomaterials.* **16**: 25–31. 1995. [[Medline](#)] [[CrossRef](#)]
 28. Eppley BL, Morales L, Wood R, Pensler J, Goldstein J, Havelik RJ, Habal M, Losken A, Williams JK, Burstein F, Rozzelle AA, and Sadove AM. Resorbable PLLA-PGA plate and screw fixation in pediatric craniofacial surgery: clinical experience in 1883 patients. *Plast Reconstr Surg.* **114**: 850–856, discussion 857. 2004. [[Medline](#)] [[CrossRef](#)]
 29. Neuendorf RE, Saiz E, Tomsia AP, and Ritchie RO. Adhesion between biodegradable polymers and hydroxyapatite: Relevance to synthetic bone-like materials and tissue engineering scaffolds. *Acta Biomater.* **4**: 1288–1296. 2008. [[Medline](#)] [[CrossRef](#)]
 30. Ramot Y, Haim-Zada M, Domb AJ, and Nyska A. Biocompatibility and safety of PLA and its copolymers. *Adv Drug Deliv Rev.* **107**: 153–162. 2016. [[Medline](#)] [[CrossRef](#)]
 31. Ramot Y, Nedvetzki S, Rosenfeld S, Emanuel N, and Nyska A. Toxicity and safety study of d-plex₁₀₀ in a sternal surgical defect in New Zealand White Rabbits. *Toxicol Pathol.* **47**: 504–514. 2019. [[Medline](#)] [[CrossRef](#)]
 32. Ramot Y, Nyska A, Markovitz E, Dekel A, Klaiman G, Zada MH, Domb AJ, and Maronpot RR. Long-term local and systemic safety of poly(l-lactide-co-epsilon-caprolactone) after subcutaneous and intra-articular implantation in rats. *Toxicol Pathol.* **43**: 1127–1140. 2015. [[Medline](#)] [[CrossRef](#)]